SCIENTIFIC REPORTS

OPEN

SUBJECT AREAS:
MITOTIC SPINDLE
KINESIN

Received
9 July 2013

Accepted
13 September 2013

Published
30 September 2013

Correspondence and requests for materials should be addressed to S.I. (ishiwata@waseda.jp)

* These authors contributed equally to this work.

Chromosome position at the spindle equator is regulated by chromokinesin and a bipolar microtubule array

Jun Takagi[1]*, Takeshi Itabashi[1]*, Kazuya Suzuki[1] & Shin'ichi Ishiwata[1,2]

[1]Department of Physics, Faculty of Science and Engineering, Waseda University, 3-4-1 Okubo, Shinjuku, Tokyo 169-8555, Japan, [2]Waseda Bioscience Research Institute in Singapore (WABIOS), 11 Biopolis Way, #05-01/02 Helios, Singapore 138667, Singapore.

The chromosome alignment is mediated by polar ejection and poleward forces acting on the chromosome arm and kinetochores, respectively. Although components of the motile machinery such as chromokinesin have been characterized, their dynamics within the spindle is poorly understood. Here we show that a quantum dot (Qdot) binding up to four *Xenopus* chromokinesin (Xkid) molecules behaved like a nanosize chromosome arm in the meiotic spindle, which is self-organized in cytoplasmic egg extracts. Xkid-Qdots travelled long distances along microtubules by changing several tracks, resulting in their accumulation toward and distribution around the metaphase plate. The analysis indicated that the direction of motion and velocity depend on the distribution of microtubule polarity within the spindle. Thus, this mechanism is governed by chromokinesin motors, which is dependent on symmetrical microtubule orientation that may allow chromosomes to maintain their position around the spindle equator until correct microtubule–kinetochore attachment is established.

The maintenance of chromosome alignment at the spindle equator during metaphase is an important step in precise chromosome segregation[1,2]. Recently, several works provided models of chromosomal alignment during meiosis/mitosis by showing that chromosomes move to and stay around the periphery of spindle equator (prometaphase-belt or chromosome ring) before bi-orientation[3,4]. It was known that the plus-end-directed motors, chromokinesins, which attach primarily to chromosome arms, contribute to the lateral sliding of chromosomes toward the equatorial belt[5,6]. In the kinetochores, another plus-end-directed kinetochore motor, CENP-E, plays an essential role in the alignment of chromosomes[7]. Although these studies show how chromosomes reach the equator and reach bi-orientation, the question of how chromosomes keep their position at the equator without either polar ejection or poleward forces until the bi-orientation is established remains poorly understood.

Chromokinesins such as kinesin-4 and Kid/kinesin-10 participate in cell division by regulating meiosis, chromosome behaviour, spindle assembly, and regulation of microtubule density[8–13]. A recent study defined the individual roles of kinesin-4 and Kid/kinesin-10 during chromosome alignment in the human mitotic spindle[14]; kinesin-4 suppresses and Kid/kinesin-10 enhances the polar ejection force. In the *Xenopus* meiotic spindle, the molecular motor Xkid/kinesin-10 directs chromosomes to the plus end of microtubules and therefore plays a crucial role in aligning chromosomes[15,16]. Although *in vitro* experiments identify Kid as a molecular motor[17–19], how its movement contributes to chromosome alignment has not been characterized within an intact spindle comprising a bipolar array of microtubules. Using self-organized meiotic metaphase spindles in *Xenopus* egg extracts, we determined how Xkid brings and maintains the chromosome arm at the metaphase plate within the meiotic spindle, depending on the distribution of polarity and length of microtubules.

Results

Xkid-Qdots traverse long distances towards the spindle equator. A cDNA comprising full-length Xkid fused to green fluorescent protein (GFP) (Xkid-GFP-FL) was used to generate Xkid-GFP-FL protein using coupled *in vitro* transcription-translation in *Xenopus* egg extracts (Supplementary Fig. S1a–c). We could then distinguish the localization of Xkid-GFP from that of endogenous Xkid in an extract containing meiotic spindles. Xkid-GFP-FL was clearly visible on chromosomes in a metaphase spindle (Fig. 1a). This localization depended on the Xkid C-terminal DNA-binding domain, because truncation of this domain (Xkid-GFP-ΔDB) broadly distributed over

the microtubules throughout the spindles (Supplementary Fig. 1d). These findings are consistent with the localization of Xkid in *Xenopus* oocytes[12] and human KID in a somatic cell[20]. To assess the effect of motor activity, we confirmed that an ATPase-deficient mutant harbouring a T125N mutation (Xkid-GFP-FL-T125N) interfered with the chromosome alignment in meiotic spindles in the presence of endogenous Xkid (Fig. 1a). This phenotype is very similar to that of spindles assembled in Xkid-depleted extracts[15]. In contrast, Xkid-GFP-ΔDB-T125N did not induce chromosome misalignment (Supplementary Fig. S1d). These results demonstrate that full-length Xkid-GFP aligns chromosomes to microtubules using the energy generated by ATP hydrolysis.

We next assessed the dynamics of Xkid within the spindle (average spindle length was 44.8 ± 1.6 μm (mean ± s.e.m., n = 9 spindles)). A number of factors made this analysis very difficult as follows: (i) fluorescence detection of single molecules of GFP in a thick spindle is prevented because of high fluorescence background, and (ii) Xkid-GFP-FL accumulates on chromosomes, so that fluorescence of molecules on the microtubules is relatively diminished (Fig. 1a). To overcome these difficulties, we performed confocal fluorescence imaging using an anti-GFP antibody bound to Qdots, which bind as many as four Xkid-GFP-FL molecules. By adding Xkid-GFP-FL bound to antibody-conjugated Qdots to extracts immediately before starting time-lapse imaging (Supplementary Fig. S1b), we successfully detected the motion of Xkid within an intact spindle (Supplementary Video S1). Xkid-Qdots were observed on chromosomes as well as on microtubules (Fig. 1b, arrows). Kid is a non-processive motor, but multiple Kid molecules can work as an ensemble to exert their functional roles on microtubules[18,19]. In the absence of Xkid-GFP-FL, antibody-conjugated Qdots did not detectably bind microtubules nor move processively along the spindle (Supplementary Video S2). The present results show that an Xkid-Qdot representing an Xkid complex moved bidirectionally along the pole-to-pole axis and finally reached the chromosomal region. Although Xkid-Qdots often passed the spindle equator without binding to a chromosome, they behaved like a chromosome within the meiotic spindle by switching to the opposite direction (Fig. 1b, c).

The motility of Xkid-Qdots was analysed by tracking the position within a spindle (Figs. 1c and 2a). Xkid-Qdots moved on the microtubules and paused or switched direction (Fig. 2b), implying that Xkid-Qdots changed several tracks of microtubules aligned parallel or antiparallel. Thus, the maximum total run length was approximately 17 μm for 180 s, which is approximately equal to the distance between the spindle pole and the metaphase plate in a *Xenopus* meiotic spindle. By fitting the total run-length distribution to a single exponential, the average distance over which an Xkid-Qdot traverses continuously on the microtubules was about 5.3 μm with an average lifetime of 35 s (Fig. 2c and Supplementary Table S1). However, some Qdots deviated from the focal plane on their way to the metaphase plate. These results suggest that the run length and the lifetime of Xkid-Qdots were underestimated.

To analyse the directional movement of Xkid-Qdots, we defined three directions of movement (Fig. 2a; see Methods for details) as follows: towards the spindle equator (equator mode), towards the spindle pole (pole mode), and indistinguishable (E–P mode). Average velocities (mean ± s.e.m. nm s^{-1}) of Xkid-Qdots as determined from a single Gaussian fit of the instantaneous velocity distributions (Fig. 2d), were 136 ± 1 nm s^{-1} in the equator mode, 125 ± 1 nm s^{-1} in the pole mode and 92 ± 2 nm s^{-1} in the E–P mode, respectively (Supplementary Table S1). The velocities in the equator and pole modes were consistent with that of Kid measured *in vitro*[18,19] (140–160 nm s^{-1}) and faster than that of microtubule flux[21] (approximately 43 nm s^{-1}). The average run length during directional movement was 1–2 μm, but Xkid-Qdots moved longer distances in the equator mode than that in the pole mode (Fig. 2e and Supplementary Fig. S1e). Further, the lifetimes (average = 10–17 s) tended to be similar; that is, Xkid-Qdots in the equator mode dwelled on the microtubules for longer times than those in the pole mode (Fig. 2e and Supplementary Fig. S1f). The *Xenopus* meiotic spindle is composed of short microtubules (2–15 μm)[22]. The average run length of Xkid-Qdots in the equator mode (2.32 ± 0.18 μm (mean ± s.e.m.)) was not significantly different from the average length of microtubules, of which plus ends direct to the metaphase plate and exist between a spindle pole and an equator[22]. These results suggest

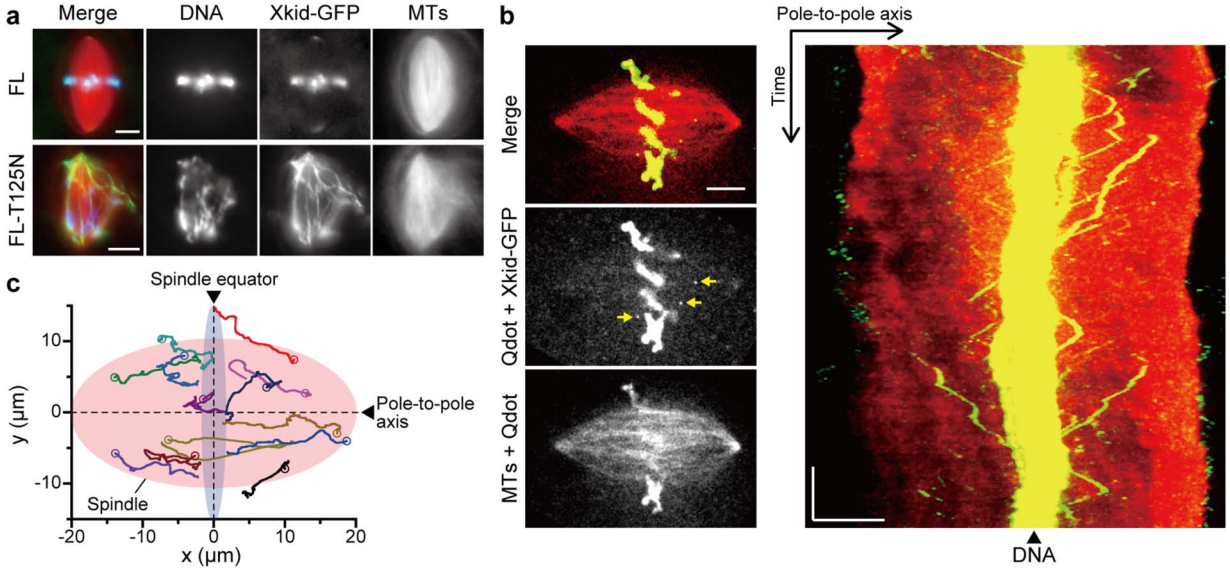

Figure 1 | Analysis of Xkid-Qdot movement within the meiotic spindle. (a) Localization of Xkid-GFP-FL and Xkid-GFP-FL-T125N in the metaphase spindle in self-organized in *Xenopus* egg extracts. The Xkid constructs are shown in green. TMR- bovine brain tubulin and 4′,6-diamidino-2-phenylindole (DAPI) were added to visualize microtubules (red) and DNA (blue), respectively. Scale bar represents 10 μm. (b) Localization and motion of Xkid-Qdots (green or yellow, when merged with red) in the spindle. Arrows indicate Xkid-Qdots moving on the spindle microtubules (red). The right panel shows a kymograph of Xkid-Qdots motion along the pole-to-pole axis of the spindle depicted on the left panels. Scale bars represent 10 μm and 100 s. (c) Trajectories of Xkid-Qdots in the spindle. Open circles indicate the initial position of trajectory.

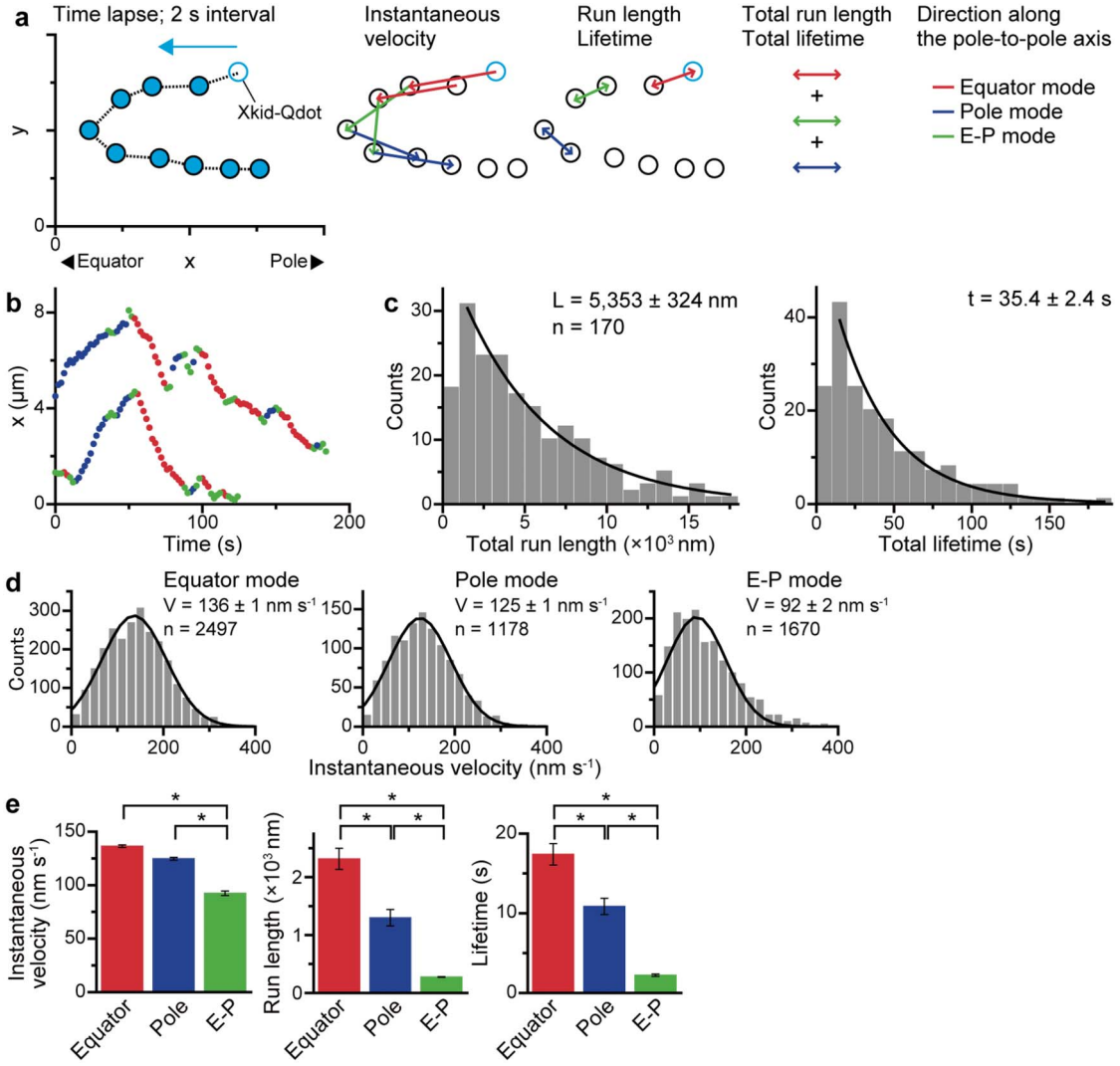

Figure 2 | Xkid-Qdots traverse long distances towards the spindle equator. (a) Schematic of the analysis of Xkid-Qdot motion. Xkid-Qdot motion was categorized into the three modes, Equator (E), Pole (P) and E-P, by the direction of movement along the pole-to-pole axis of spindle, and was analysed by calculating instantaneous velocity, run length, and lifetime in each mode, total run length, and total lifetime in each Qdot (see Methods). (b) Time course of the motion of Xkid-Qdots along the pole-to-pole axis of the spindle (n = 2 Qdots; red, equator mode; blue, pole mode; green, E-P mode). (c) Histograms of total run lengths and lifetimes for Xkid-Qdots (n = 9 spindles, 170 Qdots). The indicated average total run length (*L*) and average total lifetime (*t*) were determined by fitting the data to single exponentials excluding the first bin. (d) Histograms of instantaneous velocity for Xkid-Qdots in each mode fitted to a single Gaussian distribution (n = 9 spindles, 170 Qdots). (e) Average instantaneous velocity, run length and lifetime for Xkid-Qdots in each mode obtained by Gaussian or exponential fitting (mean ± s.e.m., data are shown in Supplementary Table S1, see also (d) and Supplementary Fig. S1e, f). Asterisks indicate the result of *t*- and the Mann-Whitney *U* tests ($p < 0.05$).

that Xkid-Qdot traverse the full length of microtubules until the plus-end tip and then translocate to another.

The motion and direction of movement of Xkid-Qdots depend on the position in the spindle along the pole-to-pole axis. To investigate the relationship between Xkid motility and spatial distribution of microtubules, the regional variation of Xkid-Qdot motility within the spindle was analysed along the spindle pole-to-pole axis (Fig. 3 and Supplementary Fig. S2a–d). Within a spindle, Xkid-Qdots, which were detected as a single fluorescent spot, mostly resided near the metaphase plate (Fig. 3a). The number of Xkid-Qdots possessing a DNA-binding domain decreased in the chromosomal region, because we could not detect an individual Qdot walking on the microtubules within a central region to which numerous chromosome-bound Qdots localized (Fig. 1b). Note that Xkid-GFP-ΔDB-Qdots were frequent around the spindle equator where chromosomes were located (Supplementary Fig. S2e,f). These results imply that the accumulation of multiple Xkid-Qdots in the metaphase plate is related neither to its DNA-binding domain nor to its binding target, the chromosome.

We asked why Xkid-Qdots move to and remain at the spindle equator. The direction that Xkid-Qdots moved depended on the region within the spindle along the pole-to-pole axis (Fig. 3b). The probability of the equator mode increased near the spindle pole, whereas there was no difference between the equator and pole modes near the metaphase plate. Xkid-Qdots moved towards the equator faster near the spindle pole than around the metaphase plate (Fig. 3c, Supplementary Fig. S3a and Table S2). In contrast, the velocity of the pole mode gradually decreased as Xkid-Qdots approached the spindle pole, and the run length and lifetime tended to decrease near the pole (Fig. 3d, Supplementary Fig. S3b,c and Table S2). Thus, the instantaneous velocity, run length, and lifetime depended on both the spindle region and the direction of movement.

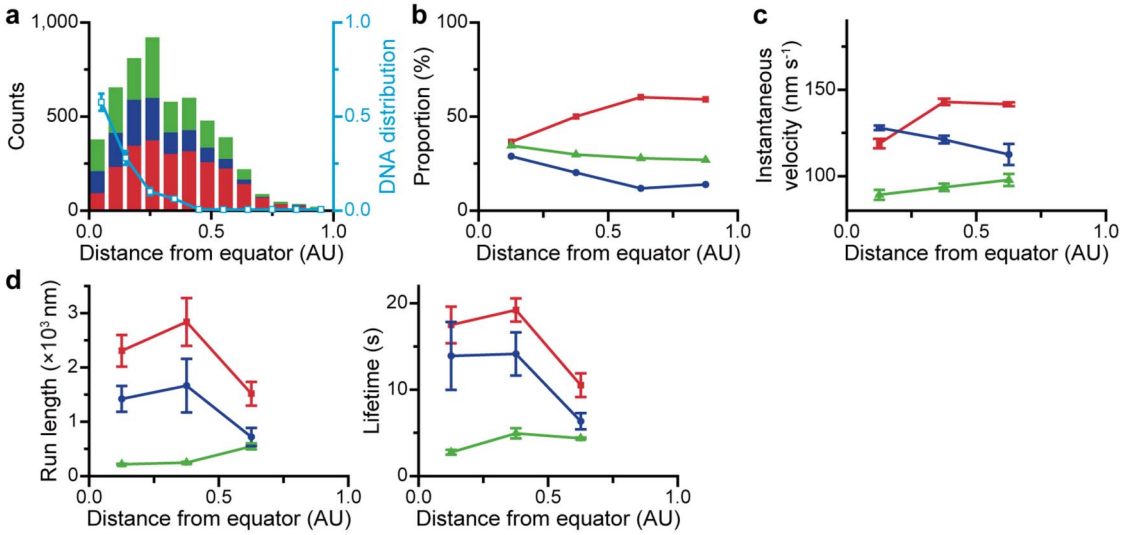

Figure 3 | The motion and direction of movement of Xkid-Qdots depend on the position in the spindle along the pole-to-pole axis. Spatial distribution of Xkid-Qdots and their motion along the pole-to-pole axis. (a) Histogram of the spatial distribution of Xkid-Qdots at each time point (red, equator mode; blue, pole mode; green, E-P mode) (n = 9 spindles, 170 Qdots, 5,234 time points) and DNA distribution along the pole-to-pole axis (mean ± s.e.m.; blue, n = 7 spindles) as a function of the distance from equator (AU). (b) Spatial distribution of the mode of motion along the pole-to-pole axis (red, equator mode; blue, pole mode; green, E-P mode) shown in (a). Each region represents at least 100 time points. (c) Spatial distribution of the instantaneous velocity along the pole-to-pole axis (mean ± s.e.m.; red, equator mode; blue, pole mode; green, E-P mode). Data with statistical significance (*p*) are shown in Supplementary Table S2, see also Supplementary Fig. S3a. (d) Spatial distribution of the run length and lifetime along the pole-to-pole axis (mean ± s.e.m.; red, equator mode; blue, pole mode; green, E-P mode). Data are shown in Supplementary Table S2, see also Supplementary Fig. S3b, c.

Previous research on the distributions of microtubule polarity and length in the *Xenopus* meiotic spindle[22,23] shows that the plus ends of microtubules direct either towards an equator or equally to a pole around the metaphase plate; however, approximately 70% of microtubules, among those located 10 μm away from the pole, direct to an equator. The regional variation in the direction of motion of Xkid-Qdots coincided with the distribution of the polarity of microtubules aligned in the spindle. Thus, approximately 83% of Xkid-Qdots, which were located 10 μm away from the pole, moved to an equator. Therefore, near the equator, Xkid-Qdots, which have multiple binding sites on microtubules, might interact more frequently with the antiparallel microtubules than moving to the equator, causing the decrease in velocity of the equator mode (Fig. 3c). In contrast, microtubules are shorter near spindle poles and longer away from them. In addition to the effect of the plus-end distribution, the abundant short microtubules near the pole could increase the frequency of changing the tracks of the Xkid-Qdots, causing the run length and lifetime to decrease (Fig. 3d). Thus, the probability of moving in a particular direction at a certain velocity likely reflects the distribution of the length and the polarity of microtubules within the spindle, suggesting that the dynamic behaviours of Xkid-Qdots are determined by the structure of the microtubule.

Xkid-Qdots accumulate towards the plus ends of microtubules in the spindle-like microtubule structure. To assess the effect of the distribution of microtubule polarity, Xkid-Qdot motility was probed in a monopolar microtubule structure prepared by adding monastrol, an inhibitor of kinesin Eg5. Approximately 80% of microtubules direct outward from the spindle pole[22] (Fig. 4a and Supplementary Video S3). In agreement with the distribution of microtubule polarity, the proportion of Xkid-Qdots moving outward from the pole (outward mode) was much larger than that moving to the pole (pole mode) throughout this monopolar structure (Fig. 4b, c). When Xkid-Qdots moved and reached the tip of astral structure, they moved back and forth and/or likely stuck to the tip (O-P mode). Although the instantaneous velocity, run length and lifetime were slightly smaller than those in a bipolar spindle (Supplementary Fig. S4a–c), these results demonstrate that the directional bias of the motion of Xkid-Qdots is enhanced by the controlled microtubule polarity.

When two monopolar structures were occasionally located nearby, a spindle-like bipolar structure was assembled (Fig. 4d and Supplementary Video S4). The distribution of microtubule polarity was maintained, so that the microtubules derived from each aster slightly crossed only at the boundary (Supplementary Fig. S4d and Supplementary Video S5). The outward mode increased far from the boundary (Fig. 4e, f), in accordance with the monopolar structure. At the boundary region, the proportion of the outward mode decreased and became nearly equal to that of the pole mode, and the proportion of O-P mode was the largest (Fig. 4f). As a result, Xkid-Qdots characteristically distributed at the boundary (Fig. 4d). Further, in a tripolar structure resembling an abnormal spindle, Xkid-Qdots accumulated at the boundaries between asters (Supplementary Fig. S4e and Supplementary Video S6). In the spindle-like structures, the crosslinking of microtubules is weak because of the inhibition of kinesin Eg5 function[24]. Therefore, the overlap length between the bidirectional microtubules was shorter, and the spacing between them might have been larger than that in the normal spindle (Supplementary Videos S4–S6). Thus, Xkid-Qdots more frequently reached the plus ends of microtubules and could change their tracks, indicating that the O-P mode may have increased with the decrease in run length and lifetime (Supplementary Fig. S4f–h).

Discussion

In meiosis and mitosis, the spatial positioning of chromosomes around the spindle equator is important for facilitating the bipolar attachment of the kinetochores to the microtubules[3,4,7]. The process governing how chromosomes congress on the equator and achieve the bidirectional attachment of kinetochore–microtubules has been extensively studied. In contrast, an intermediate process that maintains chromosome position around the spindle equator before establishing stable attachment is not well characterized[5,25,26]. Although

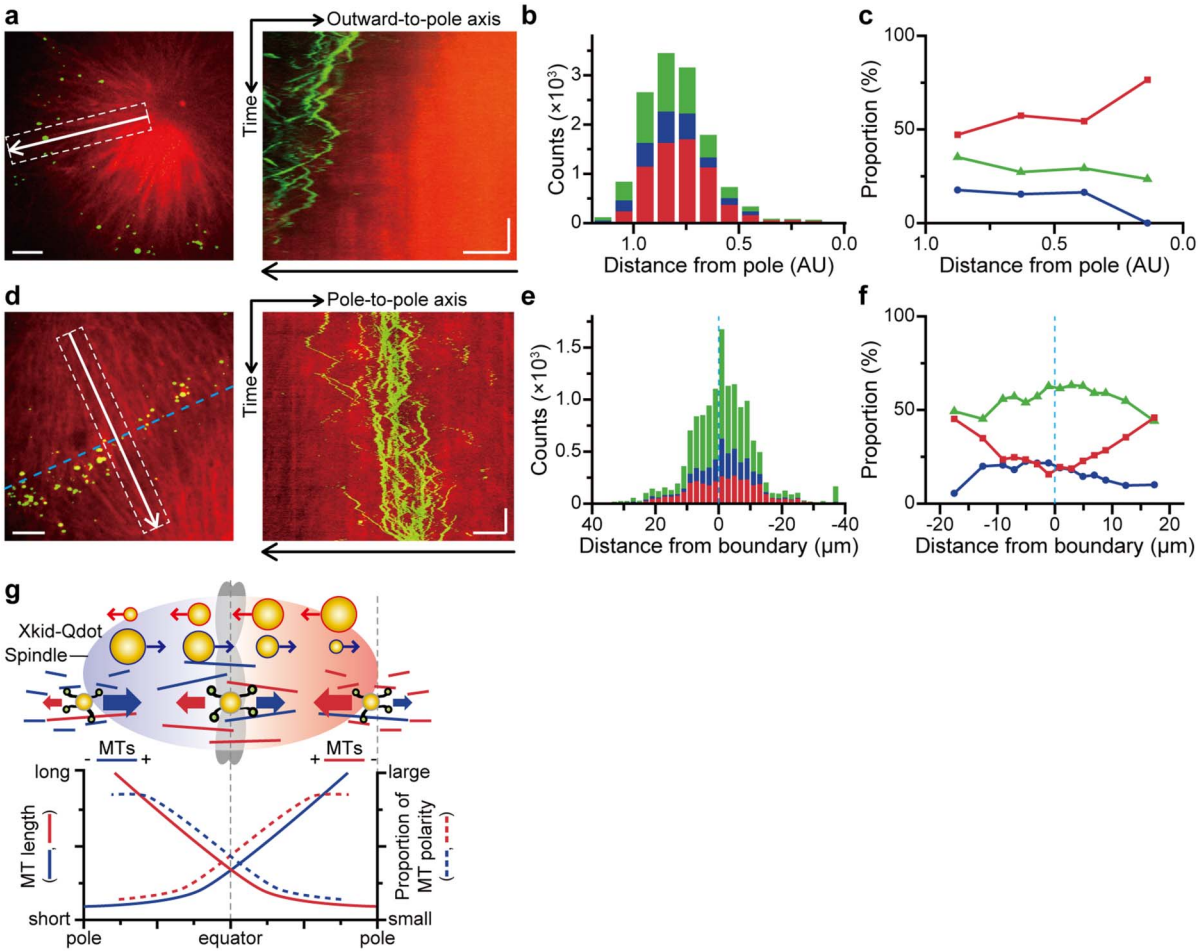

Figure 4 | Xkid-Qdots accumulate towards the plus ends of microtubules in the spindle-like microtubule structure. The monopolar microtubule structure ((a)–(c), n = 12 spindles, 569 Qdots, 12,362 time points) and the spindle-like bipolar structure ((d)–(f), n = 1 spindle, 518 Qdots, 13,792 time points) were formed in the presence of 200 μM monastrol. (a) Localization and motion of Xkid-Qdots (green) in the monopolar microtubule structure (red). The right panel shows a kymograph of Xkid-Qdot motion in a region depicted in the left panel (white dashed box) along the white arrow. (b) Histogram of spatial distribution of Xkid-Qdots in the monopolar microtubule structure for each time point from the pole to outward (red, outward mode; blue, pole mode; green, O-P mode). (c) Spatial distribution of the mode of motion in the monopolar microtubule structure from the pole to outward (red, outward mode; blue, pole mode; green, O-P mode). Each region represents at least 100 time points. (d) Localization and movement of Xkid-Qdots (green) in the spindle-like bipolar assembly of a pair of monopolar microtubule structures (red). The right panel shows a kymograph of Xkid-Qdots in a region depicted in the left panel (white dashed box) along the white arrow. (e) Histogram of spatial distribution of Xkid-Qdots in the spindle-like bipolar structure at each time point along the axis perpendicular to the blue dashed line in the left panel of (d) (red, outward mode; blue, pole mode; green, O-P mode). (f) Spatial distribution of the mode of motion in the spindle-like bipolar structure along the axis perpendicular to the blue dashed line in the left panel of (d) (red, outward mode; blue, pole mode; green, O-P mode). Each region represents at least 100 time points. (g) Schematic showing Xkid-Qdot motion along the spindle's symmetrically ordered microtubule structure. Xkid-Qdot movement along the spindle is indicated by yellow circles, and their size represents the probability of each directional movement. Dashed and solid lines represent the proportion of polarity and average length of microtubules derived from each spindle pole (red and blue), respectively. Scale bars in (a) and (d) represent 10 μm and 100 s.

multiple Xkid molecules bound to Qdot might form an oligomer and/or change molecular properties, the Xkid-Qdots described here mimic a nanosize chromosome arm, meaning that only the polar ejection force is responsible for the observed behaviours[27]. The processive behaviours of Xkid-Qdots looked similar to the motions of chromosome arms, such as the congression to and positioning around the spindle equator. The *Xenopus* meiotic spindle forms a "prometaphase belt" as observed in mouse oocytes (Supplementary Fig. S4i)[3]. This positioning of chromosomes before the formation of metaphase plate may require a chromokinesin-mediated mechanism[3,4]. Our present results demonstrate that chromokinesins serve as one of the components of the machinery required for chromosome positioning, enabling the chromosomes to maintain their position at the spindle equator without the kinetochore machinery during the transition from prometaphase to metaphase.

Our present results (summarized in Fig. 4g) suggest that the accumulation of chromokinesins is facilitated by the overlap of microtubules with equally distributed polarity at the spindle equator[22]. Thus, the micromechanical architecture of meiotic/mitotic spindle itself, which is coupled to molecular motors (kinesins, cytoplasmic dynein) and microtubule-associated proteins, may contribute to efficient chromosome alignment[25,28–30]. In conclusion, the symmetrically ordered structure of microtubules functions as a field for the molecular motors to transport the spindle components efficiently and continuously to their final destinations.

Methods

Spindle assembly in *Xenopus* egg extracts. *Xenopus* egg extracts were prepared as described previously[31]. Meiotic spindles were self-organized in the extracts with the addition of demembranated *Xenopus* sperm nuclei and tetramethylrhodamine

(TMR) (Sigma-Aldrich)-labelled tubulin (20 μg ml^{-1})[32]. To form astral structures consisting of an assembly of radially symmetric microtubules, the kinesin Eg5 inhibitor Monastrol (Sigma-Aldrich) was added (200 μM) to the extract during spindle assembly. All experiments were carried out at 20°C ± 2°C. Recombinant EB1 was labelled with Alexa Fluor® 488 and added (10 μg ml^{-1}) to the extract for imaging of the microtubule plus ends (Supplementary Fig. S4d and Video S5).

Preparation of Xkid-Qdots. A plasmid containing full-length Xkid-GFP (Xkid-GFP-FL) used for *in vitro* mRNA synthesis[16] was a gift from H. Funabiki (Rockefeller University). Xkid-GFP lacking the Xkid DNA-binding domain (Xkid-GFP-ΔDB, amino acid residues 1–504) and T125N mutants were generated using PCR mutagenesis (TOYOBO). The mRNAs encoding Xkid-GFPs were synthesized using the mMessage mMachine SP6 Kit (Ambion)[33]. *In vitro*-transcribed mRNA (0.1 mg ml^{-1}) was mixed with extract and incubated for 3 h. The extract containing expressed Xkid-GFP proteins (10% v/v) was mixed with the spindle-assembled extract 30 min before fixation for the localization analysis.

To prepare Xkid-Qdots for time-lapse fluorescence experiments, conjugation of anti-GFP antibody (Roche) to Qdots was performed using a Qdot 655 Antibody Conjugation Kit (Invitrogen). Antibody-conjugated Qdots (20–40 nM) and the extract containing Xkid-GFP proteins (~2% v/v) were added to the extract containing meiotic spindles immediately prior to making an observation chamber (Supplementary Fig. S1b). Expression of all constructs was determined by Western blot analysis using anti-GFP antibody (Roche) (Supplementary Fig. S1c), which is identical to that conjugated to Qdots for the imaging experiments.

Microscopy and live imaging. For localization of Xkid–GFP, meiotic spindles (Fig. 1a and Supplementary Fig. S1d) were fixed in 4% formaldehyde as previously described[31], and images were acquired using an upright microscope visible light (Axio Imager, Carl Zeiss) equipped with a 40 × objective (0.75 NA, Carl Zeiss) and a camera (AxioCam MRm, Carl Zeiss). For time-lapse fluorescence experiments, the egg extract containing meiotic spindles was transferred to a siliconized coverslip (custom ordered, Matsunami Glass) coated with Pluronic F-127 as described previously[34]. The fluorescence images of microtubules and Xkid–Qdots were acquired using an electron multiplying charge-coupled device (EM-CCD) camera (iXon EM+, Andor Technology) attached to an inverted microscope (IX 71, Olympus) with a 60× PlanSApo objective (1.35 NA, Olympus) and confocal scanner unit (CSU10, Yokogawa). Time-lapse images were acquired at 2 s intervals using Andor iQ software (Andor Technology).

Qdot track and motion analysis. ImageJ software (http://rsb.info.nih.gov/ij/) was used to determine the position of the spindle pole from the fluorescence image of TMR-tubulin. DNA distribution was determined from the binarized fluorescence image of Qdots attached to DNA. The positions of the Qdots were detected and tracked using the G-Track software (G-Angstrom) or a Particle Track and Analysis plugin for ImageJ. The motion of the Qdot was analysed using custom Microsoft Excel macros.

For normal bipolar spindles, (x_{tk}, y_{tk}), the position of a Qdot at time $t = t_k$, was defined by the pole-to-pole axis (x-axis) (x = 0 at the equator), and the axis perpendicular to the x-axis (y-axis; y = 0 crossing x-axis at x = 0). For monopolar microtubule structures, the origin of coordinates was defined by the position of the pole. For spindle-like bipolar structures, which were formed by the overlap of two monopolar structures, the y-axis was defined as the boundary of two asters (Fig. 4d, blue dashed line) and its perpendicular axis (x axis) (x = 0 at the boundary). Instantaneous velocity (Ins. Vel.) was defined as

$$\mathrm{Ins.Vel.}(t_k) = \frac{\sqrt{(x_{tk+2} - x_{tk})^2 + (y_{tk+2} - y_{tk})^2}}{2\tau},$$

where τ represents the time interval of the image acquisition ($\tau = t_{k+1} - t_k$). Instantaneous direction (Ins. Dir.) was defined as

$$\mathrm{Ins.Dir.}(t_k) = \begin{cases} \textit{Equator} & \text{when } |x_{tk+2}| - |x_{tk}| < 0 \\ \textit{Pole} & \text{when } |x_{tk+2}| - |x_{tk}| > 0 \end{cases}$$

in the case of normal bipolar spindle,

$$\mathrm{Ins.Dir.}(t_k) = \begin{cases} \textit{Outward} & \text{when } \sqrt{(x_{tk+2})^2 + (y_{tk+2})^2} - \sqrt{(x_{tk})^2 + (y_{tk})^2} > 0 \\ \textit{Pole} & \text{when } \sqrt{(x_{tk+2})^2 + (y_{tk+2})^2} - \sqrt{(x_{tk})^2 + (y_{tk})^2} > 0 \end{cases}$$

in the monopolar microtubule structure, and

$$\mathrm{Ins.Dir.}(t_k) = \begin{cases} \textit{Outward} & \text{when } |x_{tk+2}| - |x_{tk}| < 0 \\ \textit{Pole} & \text{when } |x_{tk+2}| - |x_{tk}| > 0 \end{cases}$$

in the spindle-like bipolar structure. The direction of Qdot (Dir. (t_k)) was defined as Ins. Dir. (t_k) when the equation,

$$\mathrm{Ins.Dir.}(t_k) = \mathrm{Ins.Dir.}(t_{k+1}) = \mathrm{Ins.Dir.}(t_{k+2})$$

was fulfilled. When the above equation was not fulfilled, the direction of Qdot was defined as E-P (O-P) (Dir. (t_k) = E-P (O-P)). In the present study, the direction of motion of Xkid-Qdots was defined not by Ins. Dir. but by Dir. When $\mathrm{Dir.}(t_{k-1}) \neq \mathrm{Dir.}(t_k) = \mathrm{Dir.}(t_{k+1}) = \cdots = \mathrm{Dir.}(t_{k+l}) \neq \mathrm{Dir.}(t_{k+l+1})$ $(l \geq 1)$, run length and lifetime were defined as

$$\text{Run length}(t_k \sim t_{k+l}) = \sqrt{(x_{tk+l} - x_{tk})^2 + (y_{tk+l} - y_{tk})^2}$$

and

$$\text{Lifetime}(t_k \sim t_{k+l}) = t_{k+l} - t_k,$$

respectively. Total run length and total lifetime were calculated by adding together the run length and lifetime in the trajectory of the same Qdot, respectively.

The statistical significance of the experimental data was determined using an unpaired two-tailed Student's *t*-test for instantaneous velocity and the Mann-Whitney *U* test for run length and lifetime with a significance level of 0.05 calculated using Origin 8.1 software (Originlab).

1. Scholey, J. M., Brust-Mascher, I. & Mogilner, A. Cell division. *Nature* **422**, 746–752 (2003).
2. Rajagopalan, H. & Lengauer, C. Aneuploidy and cancer. *Nature* **432**, 338–341 (2004).
3. Kitajima, T. S., Ohsugi, M. & Ellenberg, J. Complete kinetochore tracking reveals error-prone homologous chromosome biorientation in mammalian oocytes. *Cell* **146**, 568–581 (2011).
4. Magidson, V. *et al.* The spatial arrangement of chromosomes during prometaphase facilitates spindle assembly. *Cell* **146**, 555–567 (2011).
5. Walczak, C. E., Cai, S. & Khodjakov, A. Mechanisms of chromosome behaviour during mitosis. *Nat. Rev. Mol. Cell Biol.* **11**, 91–102 (2010).
6. Rieder, C. L. & Salmon, E. D. Motile kinetochores and polar ejection forces dictate chromosome position on the vertebrate mitotic spindle. *J. Cell Biol.* **124**, 223–233 (1994).
7. Kapoor, T. M. *et al.* Chromosomes can congress to the metaphase plate before biorientation. *Science* **311**, 388–391 (2006).
8. Castoldi, M. & Vernos, I. Chromokinesin Xklp1 contributes to the regulation of microtubule density and organization during spindle assembly. *Mol. Biol. Cell* **17**, 1451–1460 (2006).
9. Mazumdar, M. & Misteli, T. Chromokinesins: multitalented players in mitosis. *Trends Cell Biol.* **15**, 349–355 (2005).
10. Ohsugi, M. *et al.* Kid-mediated chromosome compaction ensures proper nuclear envelope formation. *Cell* **132**, 771–782 (2008).
11. Wandke, C. *et al.* Human chromokinesins promote chromosome congression and spindle microtubule dynamics during mitosis. *J. Cell Biol.* **198**, 847–863 (2012).
12. Perez, L. H., Antonio, C., Flament, S., Vernos, I. & Nebreda, A. R. Xkid chromokinesin is required for the meiosis I to meiosis II transition in Xenopus laevis oocytes. *Nat. Cell Biol.* **4**, 737–742 (2002).
13. Levesque, A. A. & Compton, D. A. The chromokinesin Kid is necessary for chromosome arm orientation and oscillation, but not congression, on mitotic spindles. *J. Cell Biol.* **154**, 1135–1146 (2001).
14. Stumpff, J., Wagenbach, M., Franck, A., Asbury, C. L. & Wordeman, L. Kif18A and chromokinesins confine centromere movements via microtubule growth suppression and spatial control of kinetochore tension. *Dev. Cell* **22**, 1017–1029 (2012).
15. Antonio, C. *et al.* Xkid, a chromokinesin required for chromosome alignment on the metaphase plate. *Cell* **102**, 425–435 (2000).
16. Funabiki, H. & Murray, A. W. The Xenopus chromokinesin Xkid is essential for metaphase chromosome alignment and must be degraded to allow anaphase chromosome movement. *Cell* **102**, 411–424 (2000).
17. Shiroguchi, K., Ohsugi, M., Edamatsu, M., Yamamoto, T. & Toyoshima, Y. Y. The second microtubule-binding site of monomeric kid enhances the microtubule affinity. *J. Biol. Chem.* **278**, 22460–22465 (2003).
18. Yajima, J. *et al.* The human chromokinesin Kid is a plus end-directed microtubule-based motor. *EMBO J.* **22**, 1067–1074 (2003).
19. Bieling, P., Kronja, I. & Surrey, T. Microtubule motility on reconstituted meiotic chromatin. *Curr. Biol.* **20**, 763–769 (2010).
20. Tokai-Nishizumi, N., Ohsugi, M., Suzuki, E. & Yamamoto, T. The chromokinesin Kid is required for maintenance of proper metaphase spindle size. *Mol. Biol. Cell* **16**, 5455–5463 (2005).
21. Yang, G., Cameron, L. A., Maddox, P. S., Salmon, E. D. & Danuser, G. Regional variation of microtubule flux reveals microtubule organization in the metaphase meiotic spindle. *J. Cell Biol.* **182**, 631–639 (2008).
22. Brugues, J., Nuzzo, V., Mazur, E. & Needleman, D. J. Nucleation and transport organize microtubules in metaphase spindles. *Cell* **149**, 554–564 (2012).
23. Heald, R., Tournebize, R., Habermann, A., Karsenti, E. & Hyman, A. Spindle assembly in Xenopus egg extracts: respective roles of centrosomes and microtubule self-organization. *J. Cell Biol.* **138**, 615–628 (1997).
24. Kapoor, T. M., Mayer, T. U., Coughlin, M. L. & Mitchison, T. J. Probing spindle assembly mechanisms with monastrol, a small molecule inhibitor of the mitotic kinesin, Eg5. *J. Cell Biol.* **150**, 975–988 (2000).
25. McIntosh, J. R., Molodtsov, M. I. & Ataullakhanov, F. I. Biophysics of mitosis. *Q. Rev. Biophys.* **45**, 147–207 (2012).
26. Dumont, J. & Desai, A. Acentrosomal spindle assembly and chromosome segregation during oocyte meiosis. *Trends Cell Biol.* **22**, 241–249 (2012).
27. Rieder, C. L., Davison, E. A., Jensen, L. C., Cassimeris, L. & Salmon, E. D. Oscillatory movements of monooriented chromosomes and their position relative

to the spindle pole result from the ejection properties of the aster and half-spindle. *J. Cell Biol.* **103**, 581–591 (1986).
28. Meunier, S. & Vernos, I. Microtubule assembly during mitosis – from distinct origins to distinct functions? *J. Cell Sci.* **125**, 2805–2814 (2012).
29. Shimamoto, Y., Maeda, Y. T., Ishiwata, S., Libchaber, A. J. & Kapoor, T. M. Insights into the micromechanical properties of the metaphase spindle. *Cell* **145**, 1062–1074 (2011).
30. Walczak, C. E. & Heald, R. Mechanisms of mitotic spindle assembly and function. *Int. Rev. Cytol.* **265**, 111–158 (2008).
31. Desai, A., Murray, A., Mitchison, T. J. & Walczak, C. E. The use of Xenopus egg extracts to study mitotic spindle assembly and function in vitro. *Methods Cell Biol.* **61**, 385–412 (1999).
32. Hyman, A. *et al.* Preparation of modified tubulins. *Methods Enzymol.* **196**, 478–485 (1991).
33. Tseng, B. S., Tan, L., Kapoor, T. M. & Funabiki, H. Dual detection of chromosomes and microtubules by the chromosomal passenger complex drives spindle assembly. *Dev. Cell* **18**, 903–912 (2010).
34. Gatlin, J. C., Matov, A., Danuser, G., Mitchison, T. J. & Salmon, E. D. Directly probing the mechanical properties of the spindle and its matrix. *J. Cell Biol.* **188**, 481–489 (2010).

Acknowledgements

We gratefully acknowledge H. Funabiki and T. M. Kapoor for providing the Xkid-GFP plasmid and advice on its use, and Y. Arai for providing a plugin for ImageJ used for the particle track and analysis. We thank Y. Abe and S. Yatabe for their preliminary experiments. This work was supported by a Research Fellowship for Young Scientists (DC1) (to J.T.), a Grant-in-Aid for Scientific Research (C) (to T.I.), and Grants-in-Aid for Specially Promoted Research and Scientific Research (S) (to S.I.) from the Ministry of Education, Culture, Sports, Science and Technology of Japan.

Author contributions

J.T. and T.I. designed and carried out the experiments. J.T. performed the data analysis. K.S. provided experimental assistance. J.T., T.I. and S.I. wrote the manuscript. All authors discussed the results and commented on the manuscript.

Additional information

Supplementary information accompanies this paper at http://www.nature.com/scientificreports

Competing financial interests: The authors declare no competing financial interests.

How to cite this article: Takagi, J., Itabashi, T., Suzuki, K. & Ishiwata, S. Chromosome position at the spindle equator is regulated by chromokinesin and a bipolar microtubule array. *Sci. Rep.* **3**, 2808; DOI:10.1038/srep02808 (2013).